

METIS: a novel coronagraph design for the Solar Orbiter mission

Silvano Fineschi^a, Ester Antonucci^a, Giampiero Naletto^b, Marco Romoli^c, Daniele Spadaro^d, Gianalfredo Nicolini^a, Lucia Abbo^a, Vincenzo Andretta^c, Alessandro Bemporad^a, Arkadiusz Berlicki^f, Gerardo Capobianco^a, Giuseppe Crescenzo^a, Vania Da Deppo^g, Mauro Focardi^c, Federico Landini^c, Giuseppe Massone^a, Marco A. Malvezzi^h, J. Dan Mosesⁱ, Piergiorgio Nicolosi, Maurizio Pancrazzi^c, Maria-Guglielmina Pelizzo, Luca Poletto, Udo H. Schühle^m, Sami K. Solanki^m, Daniele, Telloni^a, Luca Teriaca^m, Michela Uslenghi^l

^aINAF – Astrophysical Observatory of Torino, Italy, INAF - ^bUniversity of Padova – DEI, Italy;

^cUniversity of Florence, Italy; ^dINAF - Osservatorio Astrofisico di Catania (Italy);-

^eINAF - Osservatorio Astronomico di Capodimonte (Italy);-

^fAstronomical Institute of the Acad.of Sciences, (Czech Republic);

^gConsiglio Nazionale delle Ricerche (Italy); ^hUniversity of Pavia (Italy);

ⁱU.S. Naval Research Laboratory (USA); ^lINAF-IASF Milano, Italy;

^mMax-Planck-Institute für Sonnensystemforschung, Germany;

ABSTRACT

METIS (Multi Element Telescope for Imaging and Spectroscopy) METIS, the “Multi Element Telescope for Imaging and Spectroscopy”, is a coronagraph selected by the European Space Agency to be part of the payload of the Solar Orbiter mission to be launched in 2017. The mission profile will bring the Solar Orbiter spacecraft as close to the Sun as 0.3 A.U., and up to 35° out-of-ecliptic providing a unique platform for helio-synchronous observations of the Sun and its polar regions. METIS coronagraph is designed for multi-wavelength imaging and spectroscopy of the solar corona. This presentation gives an overview of the innovative design elements of the METIS coronagraph. These elements include: i) multi-wavelength, reflecting Gregorian-telescope; ii) multilayer coating optimized for the extreme UV (30.4 nm, HeII Lyman- α) with a reflecting cap-layer for the UV (121.6 nm, HI Lyman- α) and visible-light (590-650); iii) inverse external-occulter scheme for reduced thermal load at spacecraft peri-helion; iv) EUV/UV spectrograph using the telescope primary mirror to feed a 1st and 4th-order spherical varied line-spaced (SVLS) grating placed on a section of the secondary mirror; v) liquid crystals electro-optic polarimeter for observations of the visible-light K-corona. The expected performances are also presented.

Keywords: Solar instrumentation, Coronagraphy, UV imaging, UV Spectrography., visible-light polarimetry

1. INTRODUCTION

Solar Orbiter [1] is one of the Medium-class missions selected for launch by ESA in the framework of the Cosmic Vision 2015-2025 program (with Euclid), aimed to study the Sun and the inner heliosphere, with a payload made up of scientific instrumentation specifically designed to identify the origins and causes of the solar wind, the solar energetic particles, the transient interplanetary disturbances, and the heliospheric and Sun's magnetic field.

Solar Orbiter will provide the next major step forward in the exploration of the Sun and the heliosphere after the successful ESA missions Ulysses and SOHO, as well as the NASA missions TRACE, RHESSI, STEREO and SDO, and the ISAS mission, Hinode. It will be a key element of the International Living with a Star program, focused on the space research that has the objective of understanding the processes governing the connected Sun-heliosphere system.

Solar Orbiter will be launched from the Kennedy Space Center on January 2017 (nominal launch date) and after a cruise phase lasting approximately three years it will start its 7.5 years-long nominal mission phase during which it will orbit the Sun in about six months and will achieve perihelion distances down to 0.28 AU, getting closer to the Sun than any previous spacecraft. Solar Orbiter will be in a privileged position suitable to perform unprecedented scientific observations thanks to a powerful combination of in-situ and remote sensing instrumentation. Thanks to regular gravity-assist maneuvers at Venus the orbit will be tilted bringing the spacecraft to increasingly higher latitudes, allowing a view of the Sun's polar regions from latitudes higher than 30 degrees (up to 34° close to the end of the mission). Moreover, Solar Orbiter will be almost co-rotating with the Sun for a part of its orbit, providing for the first time the capability of remote-sensing solar storms and coronal eruptions building up and development over an extended period (several days) from the same viewpoint.

Solar Orbiter will perform in-situ measurements of the solar wind plasma, fields, waves, and energetic particles in a region where they are still relatively unaltered and have not had their properties modified by dynamical evolution during their propagation. Moreover, remote-sensing instrumentation will carry out simultaneous, high-resolution imaging and spectroscopic observations both in and out of the ecliptic plane, allowing connecting the in-situ measurements back to their source regions and structures.

Due to the peculiar orbit of the satellite, however, the characteristics of the environment in which it shall operate heavily affect the design of its payload, which has to withstand the harsh environment and extreme temperatures

2. METIS EXPERIMENT OVERVIEW

METIS, the *Multi Element Telescope for Imaging and Spectroscopy*, is one of the remote-sensing instruments of Solar Orbiter consisting in an innovative coronagraph for the study and overall characterization of the solar corona ([2], [3], [4], [5]). METIS is an inverted-occultation coronagraph that will image the solar corona in three different wavelengths (visible light between 590 and 650 nm, and the two Lyman- α lines of hydrogen and helium, HI at 121.6 nm and HeII at 30.4 nm) by a combination of multilayer mirror coatings and spectral bandpass filters (Figure 1).

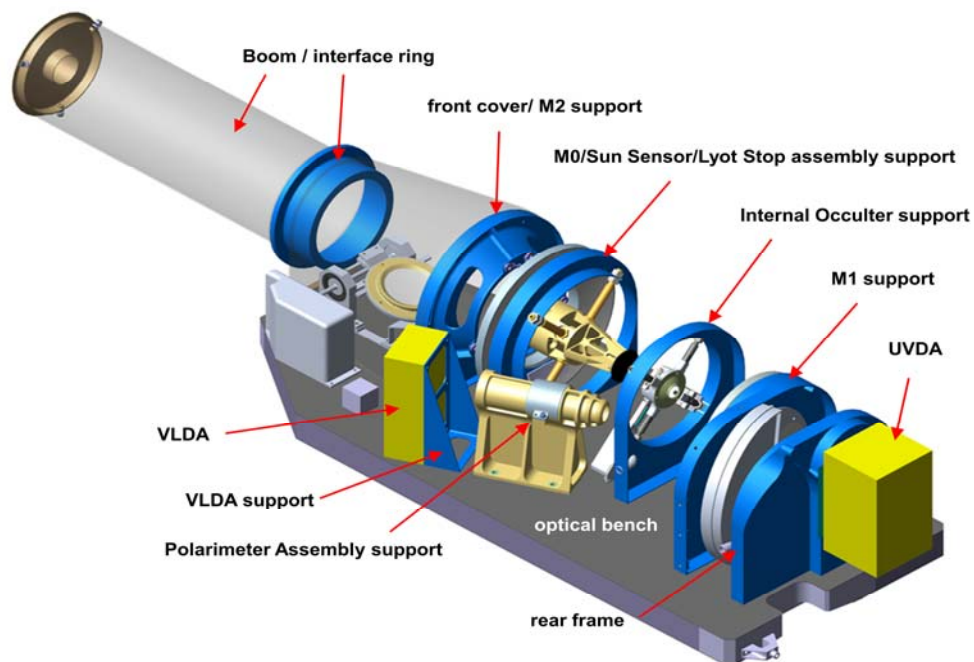


Figure 1 METIS opto-mechanical layout showing the main telescope elements [courtesy of Thales Alenia Space Italia].

The visible channel also includes a polarimeter to observe the linearly polarized component of the K corona. In addition, METIS will have the capability of collecting spectra of the HI and HeII Lyman lines simultaneously at three different heights (accomplished by a multiple slit) in a 32° angular sector of the corona (Figure 2).

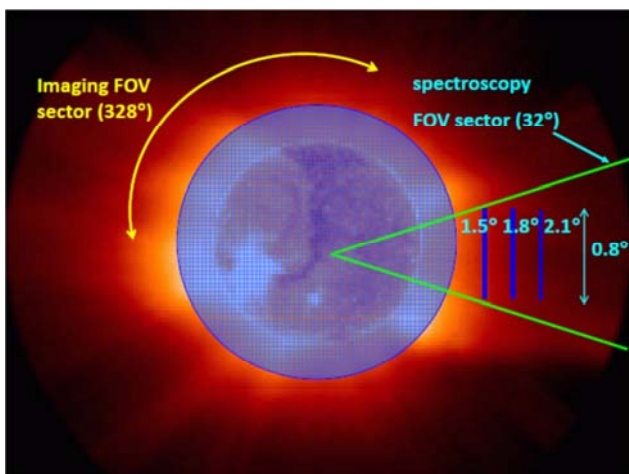


Figure 2 Imaging and spectrographic multi-slits field-of-view (FOV) at 0.28 AU for the EUV/UV spectroscopic path. The FOV sector for spectroscopy is about 32°. The remaining FOV is used for imaging in the three wavelength bands: 30.4 nm, 121.6 nm, visible-light.

These measurements will allow a complete characterization of the three most important plasma components of the corona and the solar wind: electrons, protons, and helium.

The METIS experiment has been conceived to perform off-limb and near-Sun coronagraphy, with the goal of addressing three key scientific issues concerning:

- the origin and heating/acceleration of the fast and slow solar wind streams;
- the origin, acceleration and transport of the solar energetic particles;
- the transient ejection of coronal mass (coronal mass ejections - CME's) and its evolution in the inner heliosphere.

Solar Orbiter will provide METIS with a unique platform for close-up studies of the Sun's atmosphere and of its polar regions. Indeed, much of the crucial physics in the formation and activity of the heliosphere takes place close to the Sun and when structures, shocks, energetic particles and solar wind reach the Earth orbit they have already evolved, and in many cases mixed so as to blur or even cancel the signatures of their origin.

2.1 Instrument requirements

METIS is designed to achieve these science goals by combining the imaging and spectroscopic capabilities of coronagraphs and spectrometers. The coronagraph can simultaneously image the visible-light and ultraviolet emission of the solar corona and diagnose, with unprecedented temporal coverage and spatial resolution the structure and dynamics of the full corona in the field-of-view (FOV) range from 1.5° to 2.9°, corresponding to 1.5 to 3.0 solar radii (R_{\odot}), at minimum perihelion (0.28 AU), and 2.6 to 5.5 R_{\odot} , at 0.5 AU. METIS will be capable of obtaining for the first time:

- simultaneous imaging of the full corona in
 - linearly polarized visible-light (590-650 nm)
 - narrow-band ultraviolet HI Lyman α (121.6 nm)
- narrow-band extreme ultraviolet He II Ly α (30.4 nm).
- spectroscopic observations of H I Lyman α and He II Lyman α in corona.

Table 1 summarizes the METIS instrument performances. The coronagraph is based on a novel design: the coronal light enters through a circular aperture acting as an inverted external occulter located on the outside panel of the S/C heat shield. The inverted external occulter is supported by a suitable truss, which protrudes from the S/C instrument bay through the heat shield.

METIS is an externally occulted coronagraph. The occultation scheme is based on an inverted external-occulter (IEO). The IEO consists of a single, small (\varnothing 40 mm) circular aperture. A small (\varnothing 71 mm) spherical mirror (M0) rejects back the disk-light through the IEO up to 1.1° (i.e., 1.17 R_{\odot} at 0.28 AU). The imaging system is an on-axis Gregorian telescope. The detailed optical design is described in the following sections. The EUV/UV and VL detectors are described in detailed in Ref. [6].

METIS Instrument Performances	
CORONAL IMAGING	
Avg. Instrumental Stray Light (B_{cor}/B_{α})	VL $<10^{-9}$ UV/EUV $<10^{-7}$
Wavelength range:	VL: 590-650 nm; UV: 121.6 ± 10 nm EUV: 30.4 ± 2 nm
Spatial resolution	20 arcsec
Field of view	1.5° - 2.9° annular, off-limb corona
CORONAL SPECTROSCOPY	
Wavelength range:	UV: 121.6 ± 0.9 nm EUV: 30.4 ± 0.22 nm
Spectral resolution	UV: 0.072 nm EUV: 0.018 nm
Spatial resolution	45 arcsec
Field of view	Slit radial positions: 1.5°, 1.8°, 2.1° Slit extension: 0.8°
GENERAL	
Telemetry rate	10 kbit/s
Data volume (compression up to 10)	26 Gb/orbit

Table 1 METIS instrument performances

3. INSTRUMENT OPTICAL DESIGN

The inverted external occulter (IEO) consists of a circular aperture on a disk kept by a cylindrical boom at 500 mm in front of the telescope. The disk-light through the IOE is rejected back by a spherical heat-rejection mirror (M0). The coronal light, on the other hand, is collected by an on-axis Gregorian telescope. The suppression of the diffracted light off the edges of the IOE and M0 is achieved, respectively, with an internal occulter (IO) and a Lyot trap (LS). Figure 3 shows a schematic layout of the inverted-occultation coronagraph.

METIS includes 4 optical paths:

1. linearly polarized visible-light (590-650 nm)
2. narrow-band ultraviolet HI Lyman α (121.6 nm)
3. narrow-band extreme ultraviolet He II Ly α (30.4 nm).
4. spectroscopic observations of H I Lyman α and He II Lyman α in corona.

The visible-light (VL) and ultraviolet UV paths are split by an UV interference filter at 12° (cfr. Figure 4). The UV-capped multilayer (ML) coatings in the primary (M1) and secondary (M2) telescope mirrors are optimized for narrow bandpass reflectivity at 30.4 nm. The ML cap-layer has good reflectivity also in the UV (122 nm) and visible-light (590-650 nm). In the extreme UV (EUV) path, the longer wavelengths are blocked by an Al filter. The UV filter selects the 122 nm UV band and reflects the VL band. In the polarimeter a broad band filter selects the VL bandpass (590-650 nm). Table 2 summarizes the instrument optical specifications. The EUV/UV and VL detectors are described in Ref. [6].

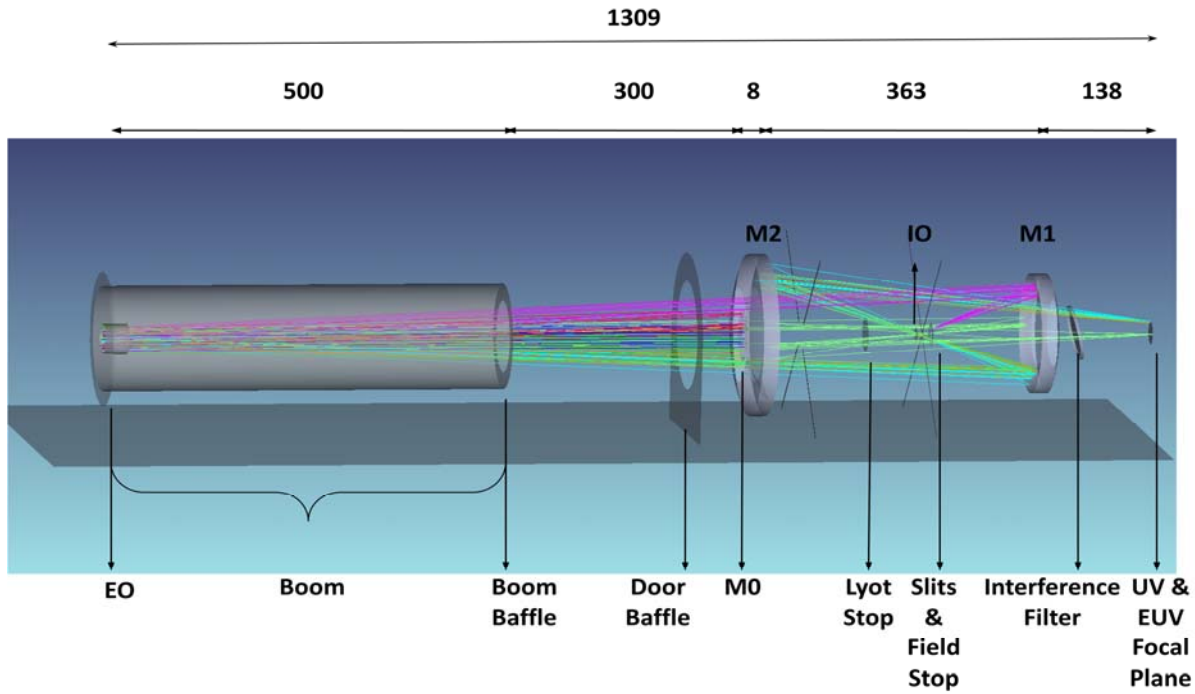


Figure 3: Optical layout of the inverted-occultation coronagraph. The telescope configuration is an externally occulted Gregorian. (dimensions are in mm).

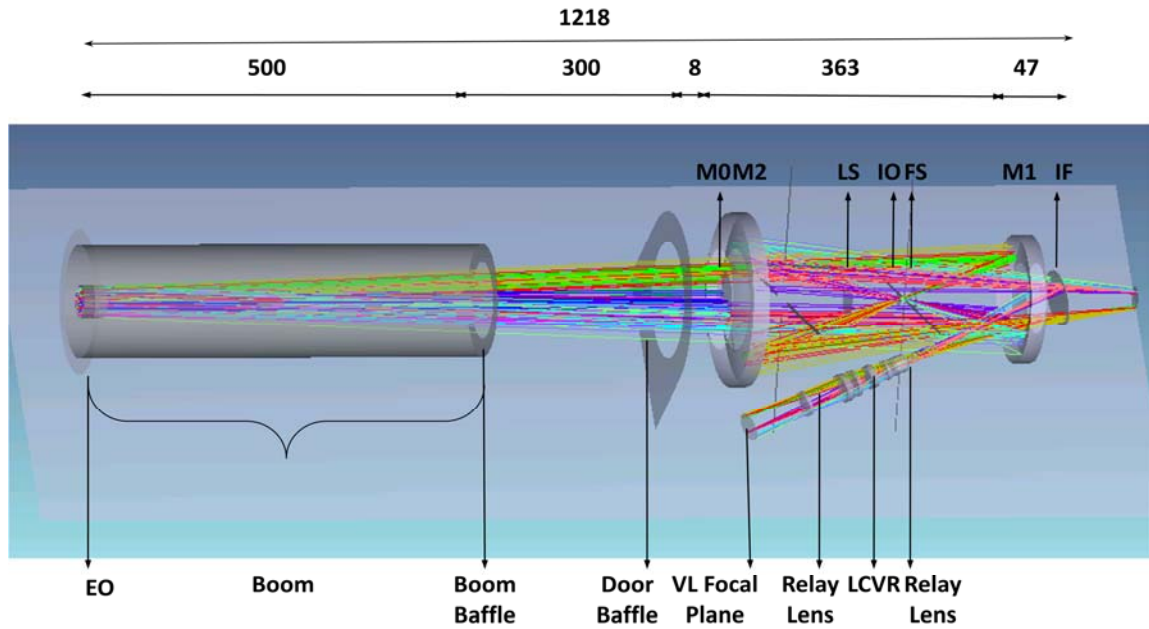


Figure 4: Optical layout of the Visible-Light and UV/EUV paths in the inverted-occultation coronagraph.

Field of View	Annular Sun-centered : 1.5° – 2.9° 1.6 – 3.1R _☉ @ 0.28 AU; 2.8 – 5.4 R _☉ @ 0.5 AU
Telescope type	Externally occulted, on-axis Gregorian
Overall length	1309 mm
Effective focal length	300 mm EUV – 296 mm UV – 360 mm Visible-light
Inverted External Occulter (IEO)	Circular hole, \varnothing : 40.0 mm
Distance EO – M0 (boom)	800.0 mm
Sun-light Rejection mirror (M0)	Spherical: \varnothing : 71.0 mm, Curvature radius: 1600.0 mm
Distance M0 - M1	370.6 mm
Primary mirror (M1)	On axis ellipsoidal: outer \varnothing : 160.0 mm, inner \varnothing 88.0 mm Curvature radius: 272.0 mm, conic: -0.662
Distance M1 - M2	363.0 mm
Secondary mirror (M2)	On axis ellipsoidal: outer \varnothing : 216.0 mm, inner \varnothing : 125.0 mm Curvature radius: 312.4 mm, conic: -0.216
Internal occulter (IO)	Distance M1 -IO: 154.8 mm; Circular: \varnothing : 5.5 mm
Lyot trap	Distance M1 – Lyot-trap: 217.9 mm; Circular obscuration: \varnothing : 46.0 mm
Dist. M2 - Focal plane	501.4 mm
Spatial resolution	VL: 20 arcsec UV and EUV: 20 arcsec \leq 2.5 R; >20 arcsec at > 2.5 R
Stray light levels	VL: $< 10^{-9}$; UV, EUV: $< 10^{-7}$
Wavelength band-pass	VL: 573-647 nm; UV HI (121.6 \pm 10) nm; EUV Hell (30.4 \pm 2) nm
Detectors	EUV/UV: IAPS; Scale factor 10.1 arcsec/pixel Image size: 30.7 mm (2048x2048) with 15 μ m pixel size VL: APS; Scale factor 10.7 arcsec/pixel Image size: 36.7 mm (2048x2048) with 18 μ m pixel size

Table 2 METIS optical specifications

3.1 UV/EUV Imaging Paths

The visible-light (VL) and EUV/UV paths are split by an UV interference filter at 12° angle of inclination with respect to the optical axis. The UV-capped multilayer (ML) coatings in the primary (M1) and secondary (M2) telescope mirrors are optimized for narrow bandpass reflectivity at 30.4 nm. The ML cap-layer has good reflectivity also in the UV (121.6 nm) and visible-light (590-650 nm). In the EUV path, the longer wavelengths are blocked by an Al filter. The UV narrow bandpass interference filter acts as VL-UV beam splitter by selecting the 121.6 nm UV band in transmission and reflecting the VL. Inside the polarimeter a broad band filter selects the VL bandpass (590-650 nm). Figure 4 shows the optical layout of the inverted-occultation coronagraph for the EUV/UV path together with the visible-light (VL) path.

The VL polarimeter includes a polarization modulation package (PMP) with a liquid crystal variable retarder (LCVR) together with a fixed quarter-wave (QW) retarder and a linear polarizer in “Senarmont” configuration ([7]). The PMP is in between a relay optics system that collimates through the PMP the linearly polarized VL from the K-corona and refocuses it on the VL detector. Figure 5 and Figure 6 show the optical performances (spot diagram and rms spot versus field-of-view, respectively) of the UV and EUV Imaging Path of the METIS coronagraph.

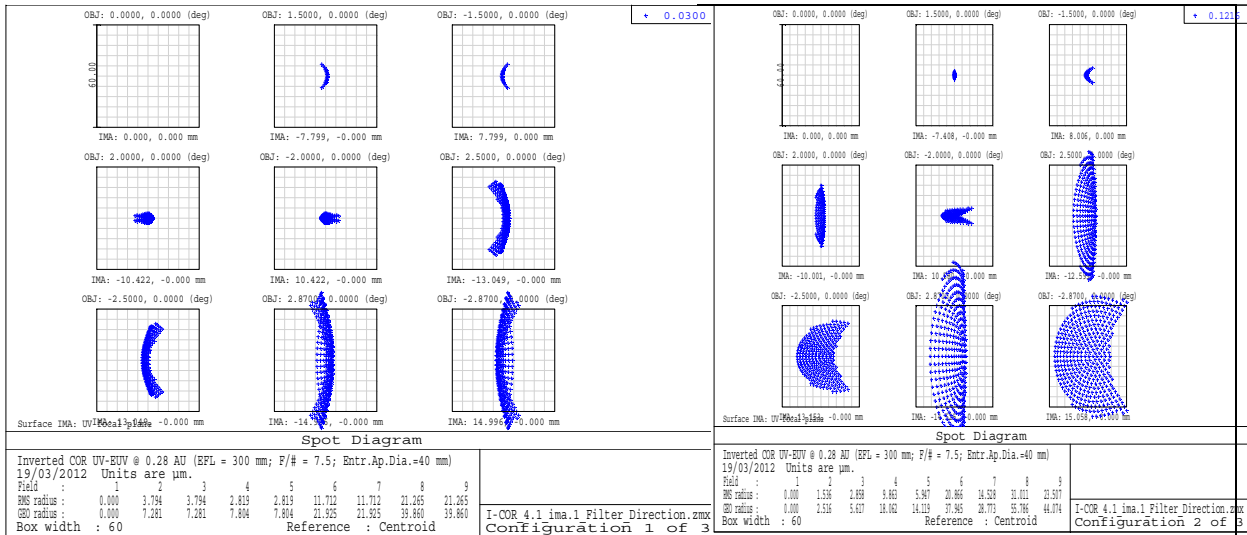


Figure 5 Left: EUV spot diagram (RMS). Right: UV spot diagrams. The box size is 30 μm

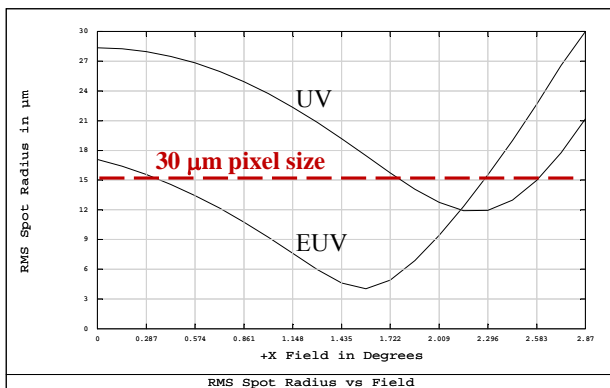


Figure 6 Geometrical UV-EUV spot size (rms) versus field-of-view

3.2 Visible-light Path and Polarimeter

The VL Path includes a polarimeter consisting of a polarimetric optical system (POS) and a relay-optics system (ROS). The ROS collimates, through the POS, the light from the image formed by the telescope on the intermediate VL focal plane (Figure 7). Then the ROS re-focuses the image on the VL detector, with a 1:1.2 magnification ratio to match the telescope plate scale with the APS pixel size. The POS electro-optically modulates the intensity of the linearly polarized K-corona. The POS is comprised of polarization optics in “Senarmont configuration”: bandpass (BP) filter (590-650 nm); fixed quarter-wave (QW) retarder; polarization modulation package (PMP) with a LCVR cell (Liquid Crystal Variable Retarder); linear polarizer (LP) ([7]). Figure 7 shows the optical layout of the VL Path. A detailed description of the VL Path is given in Ref. [8].

3.3 EUV/UV Spectrography Path

The EUV/UV spectroscopy path in METIS consists of a sector of the telescope primary mirror (M1) that is used for feeding a multi-slit spectrograph. In the spectrograph, the grating replaces a sector of the secondary mirror (M2). The grating diffracts the spectrum on the portion of the detector that is not used for coronal EUV/UV imaging. The grating is a spherical variable-line-spaced (SVLS) one with a ruling frequency of 1800 lines/mm. The SVLS grating diffracts the 30.4-nm radiation at 4th order and the 121.6-nm radiation at 1st order on the same location on the focal plane. The multi-slit input section selects a number of angular field-of-views (FOVs): 1.5°, 1.8° and 2.1° (cfr Figure 2). Figure 8 shows the optical layout of the METIS Spectrographic Path with the SVLS grating. The spectral separation between the slits is 0.44 nm at 30.4 nm, and 1.74 nm at 121.6 nm. This minimizes the overlap between the wings of spectral lines profiles in adjacent slits. Table 3 Optical specifications of the EUV/UV spectrographic path.

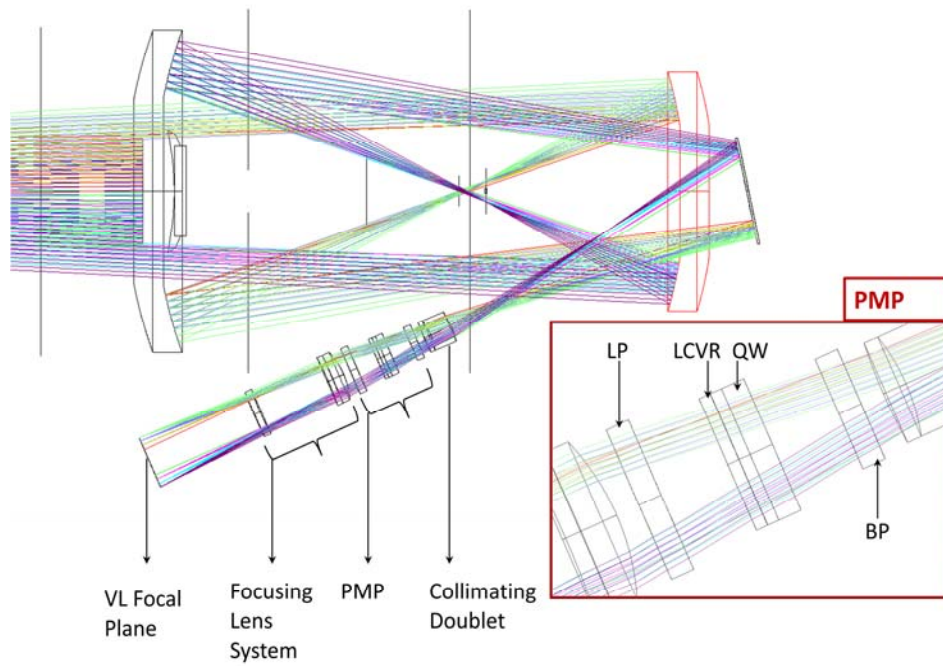


Figure 7 Optical layout of the visible light path

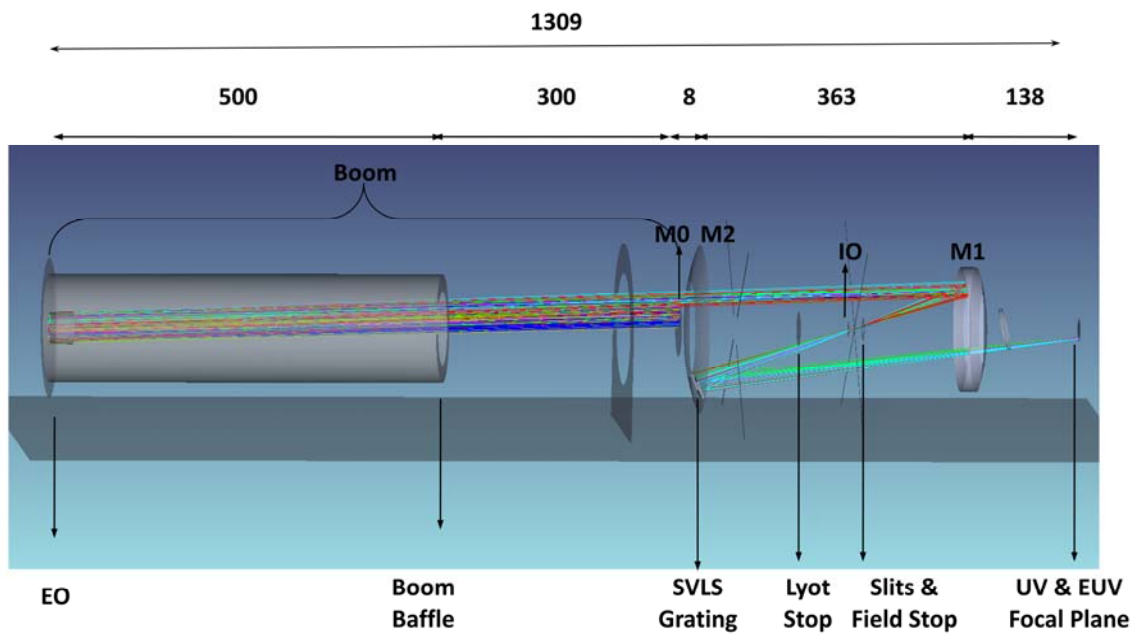


Figure 8 Optical layout of the spectrographic path with the SVLS grating (dimensions are in millimeters)

Telescope Mirror	M1 sector illuminated by the coronal light reflected into the multislit	$\pm 32^\circ$	
Spectrometer	Entrance arm	227.0 mm	
	Exit arm	500.0 mm	
	Magnification	2.2	
	Multislit (on M1 focal plane)	Slit # (FOVs)	3 (1.5°, 1.8°, 2.1°)
		Width	30 μm (FOV: 44 arcsec)
		Height (FOV)	1.5 mm ($\pm 0.3^\circ$)
Slit separation		0.72 mm	
Incidence angle (α)	$\approx 0^\circ$		
Diffraction angle (β) 4 th order of 30.4 nm, 1 st order of 121.6 nm	12.6°		
SVLS grating	Ruled area ($// \times \perp$ to grooves)	60 mm \times 23 mm	
	Radius	302.3 mm	
	Central Ruling Frequency	1800 lines/mm	
	Line Spacing Variation Factors (as defined in Zemax) T = lines/micron, y = distance from grating center (mm) $1/T = 1/T_0 + \alpha y + \beta y^2 + \gamma y^3$	T ₀	1.8
		α	2.7e-4
		β	-1.8e-6
γ		0	
Focal Plane	Pixel size	15 μm	
	Spatial Plate Scale	10 arcsec/pixel	
	Spatial Resolution (4-pixel)	41 arcsec	
	Spectral Resolution (30 μm slit-width \times 2.2 magnification)	0.018 nm (30.4 nm)	
		0.074 nm (121.6 nm)	
	Spectral separation between consecutive slits	0.45 nm at 30.4 nm	
1.8 nm at 121.6 nm			

Table 3 Optical specifications of the EUV/UV spectrographic path.

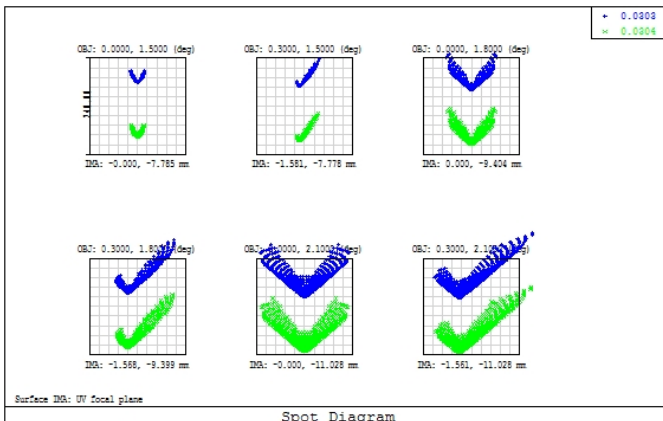


Figure 9 Spot diagrams of the HeII, 30.38 nm, and SiXI, 30.33 nm, lines on the focal plane of the spectrographic path. The spectral dispersion direction is the vertical axis. The box size is 240 μm , corresponding to 2 spectral resolution elements (slit-width's image size is 60 μm).

Figure 9 shows the optical performances (spot diagrams) of the EUV spectrograph at diffracted 4th order, 30.4 nm are very similar), together with the spectral separation between the HeII, 30.38 nm, and the SiXI, 30.33, nm lines.

The spectral resolution corresponds to the minimum spectral resolution element of 4-pixels (i.e., 0.018 nm at 30.4 nm and 0.072 nm at 121.6 nm), for the slit closest to the solar limb (1.5°) and for the intermediate slit (1.8°). For the external slit (2.1°), the spectral resolution is a factor of two lower (0.036 nm at 30.4 nm and 0.144 nm at 121.6 nm). The spatial resolution corresponds to 2 pixels (45 arcsec) for the slit closest to the disk (1.5°), to 6 pixels (~ 2 arcmin) for the intermediate slit (1.8°) and to more than 8 pixels (~ 3 arcmin) for the external slit (2.1°).

4. MULTILAYER OPTICAL COATINGS

The UV-capped multilayer (ML) coatings in the primary (M1) and secondary (M2) telescope mirrors and in the SVLS grating are optimized for narrow bandpass reflectivity at 30.4 nm. The ML cap-layer has good reflectivity also in the UV (121.6 nm) and visible-light (590-650 nm). In the EUV path, the longer wavelengths are blocked by the Al filter. The UV narrow bandpass interference filter acts as VL-UV beam splitter by selecting the 121.6 nm UV band in transmission and reflecting the VL. Inside the polarimeter a broad band filter selects the VL bandpass (590-650 nm).

The UV-capped multilayers that are currently taken into consideration for the METIS reflecting optics are ([9]):

- Standard Mo/Si (baseline coating - REF)
- ML with different capping layers (CL) materials (4 different types):
- Mo/Si + CL1 Ir/Mo
- Mo/Si + CL2 Ir/Si

The ML selection is based on the following requirements: i):high reflectivity at 30.4 nm, 121.6 nm and in the VL spectral range for simultaneous observations; ii) stability: over time (aging) –2 years shelf lifetime, 10.2 years in space; iii) thermal stability.

Table 4 summarizes the parameters of the ML samples under testing. Two types of samples of A, optimized differently: A-REF for high reflectance at 121.6 nm, A-II for high reflectance at 30.4 nm. Two samples of B1 (B1a and B1b) deposited in two different runs. This structure maximizes already the efficiency at the HeII Lyman- α line as well as the efficiency at the HI Lyman- α line.

Structure code	Capping layer structure	Periodic structure parameters
A-REF	Si (2 nm)	
A-II	Si (18.72 nm)	
B1a and B1b	Mo (3.5 nm)	d =16.4 nm
	Ir (2 nm)	$\Gamma = 0.82$
B2a and B2b	Mo (2.2 nm)	N = 30
	Ir(2 nm)	
	Si (15.4 nm)	
	Mo (2.95 nm)	

Table 4 The multilayer structures considered for METIS

A-REF and A-II are two extreme cases: A-II is optimized for maximizing the reflectivity at 30.4 nm and A-REF for maximizing the reflectivity at 121.6 nm; all intermediate results are possible; these structures therefore will have a reflectance between 20% and 22% at 30.4 nm, and between 36% and 43% at 121.6 nm. The measured and theoretical reflectivities of the ML under consideration for the METIS mirrors are reported in Table 5 ([9]):

Sample	@ 30.4 nm	@ 121.6 nm	@ 550 nm	@ 650 nm
A-REF	0.20	0.34	0.43	0.40
A-II	0.22	0.27	0.36	0.32
B1a	0.26	0.26	0.56	0.54
B1b	0.28	0.26	0.56	0.32
B2a	0.26	0.26	0.51	0.48
B2a	0.25	0.26	0.51	0.48

Table 5 Summary of the samples reflectance (black, experimental; blue, theoretical)

5. STRAY-LIGHT SUPPRESSION REQUIREMENTS

METIS is an externally occulted coronagraph. The occultation scheme is based on an inverted external-occulter (IEO). The IEO consists of a single, small (\varnothing 40 mm) circular aperture. A small (\varnothing 71 mm) spherical mirror (M0) rejects back the disk-light through the IEO up to 1.1° (i.e., $1.17 R_\odot$ at 0.28 AU, cfr. Figure 3).

The main source of stray-light in a coronagraph is the diffraction off the first element illuminated by the sun-disk light. For an externally occulted coronagraph, this is the external occulter. The diffraction off the IEO is both specularly and non-specularly reflected by the primary mirror (M1). The control of these two sources of stray-light is achieved in two ways. The diffraction off the IEO specularly reflected by M1 is suppressed by stops (i.e., internal occulter and Lyot stop); non-specularly reflected by M1 is controlled by minimizing the M1 surface roughness.

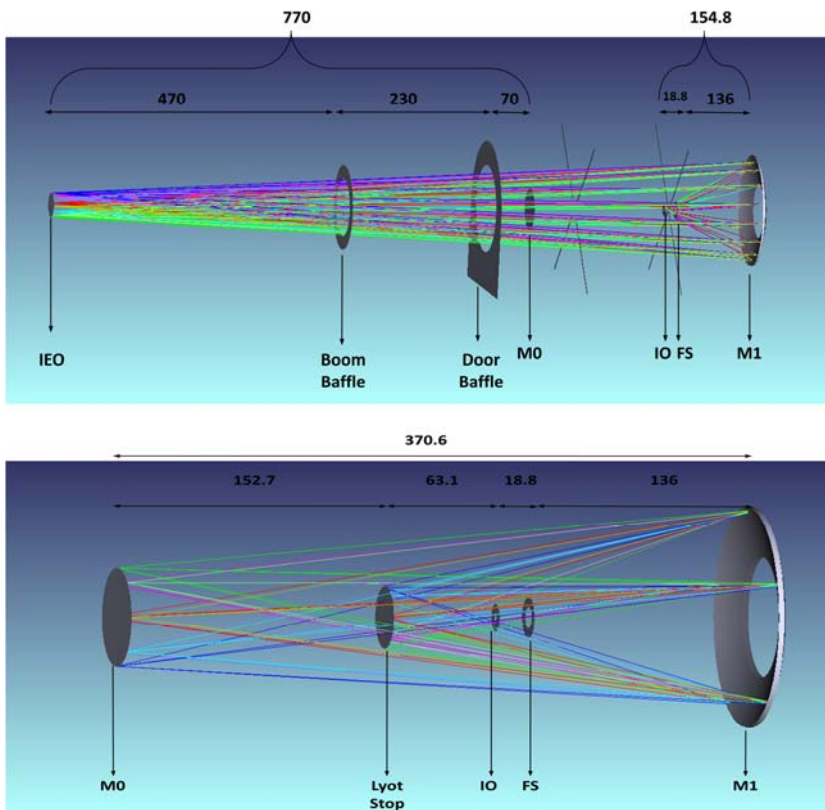


Figure 10 Top: The primary mirror M1 forms a real image of the diffracting IEO edge. This image is blocked by an internal occulter (IO). Bottom: The diffraction off IEO illuminates the edges of the disk-light rejection mirror (M0). This, in turn, diffracts the disk-light on M1. M1 creates a real image of the M0 edges that is blocked by the Lyot stop. (Dim. in mm)

frequencies that scatter the stray-light in the FOV of the field stop. Figure 11-Right shows an example of the power spectra density (PSD) as a function of spatial frequencies of a mirror's surface roughness. The level of stray-light due to the non-specularly reflected stray-light scattered off the primary mirror is estimated by convolving the energy flux diffracted on M1, shown in Figure 11-Left, by the mirror surface PSD of the type shown in Figure 11-Right. The resulting estimate of the levels of stray-light on the focal plane due to the surface roughness of the primary mirror is shown by the plots in Figure 12 ([10]).

5.1 Suppression of Specularly Reflected Diffraction

The primary mirror M1 creates a real image of the diffracting IEO edge. This image is blocked by an internal occulter (IO) stop (cfr. Figure 10-Top)

The diffraction off IEO illuminates also the edges of the disk-light rejection mirror (M0). This, in turn, diffracts the sun-light within M1's field-of-view. M1 creates a real image of the M0 edges that is blocked by the Lyot stop (Figure 10-Bottom).

5.2 Suppression of the Non-specularly Reflected Diffraction

The energy profile on the primary mirror (M1) due to visible-light diffraction off a circular aperture acting as the IEO is shown in Figure 11-Left ([10]). This energy is scattered by the surface roughness of M1 and contributes to the stray-light level on the focal plane. Thus, in order to control this source of stray-light the rms surface roughness of M1 must be minimized in the spatial

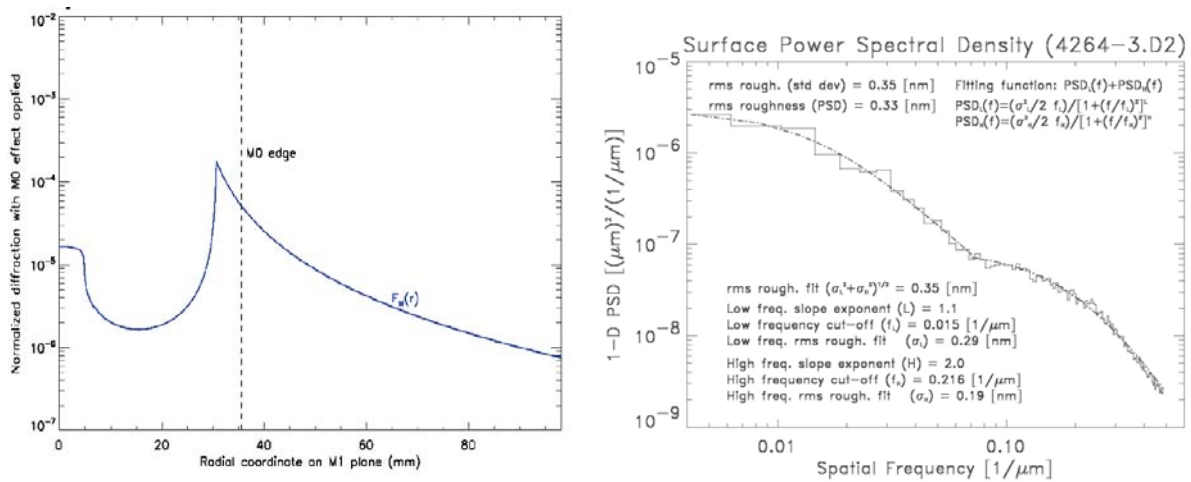


Figure 11. Left: Normalized energy flux on the M1 due to the diffraction of a circular aperture as the Inverted External Occulter. Right: Example of power spectra density versus spatial frequencies of a mirror's surface roughness

The VL estimate in Figure 12-Left includes also the additional contribution of Mie scattering due to particulate contamination of class 300 EOL. Therefore, also this additional source of non-specular stray-light needs to be controlled. According to literature and to the tests performed on a prototype of the boom occulter assembly (BOA), the optimization of the external occulter geometry (i.e., apodization) is expected to improve the stray light suppression of the instrument by more than one order of magnitude ([10]).

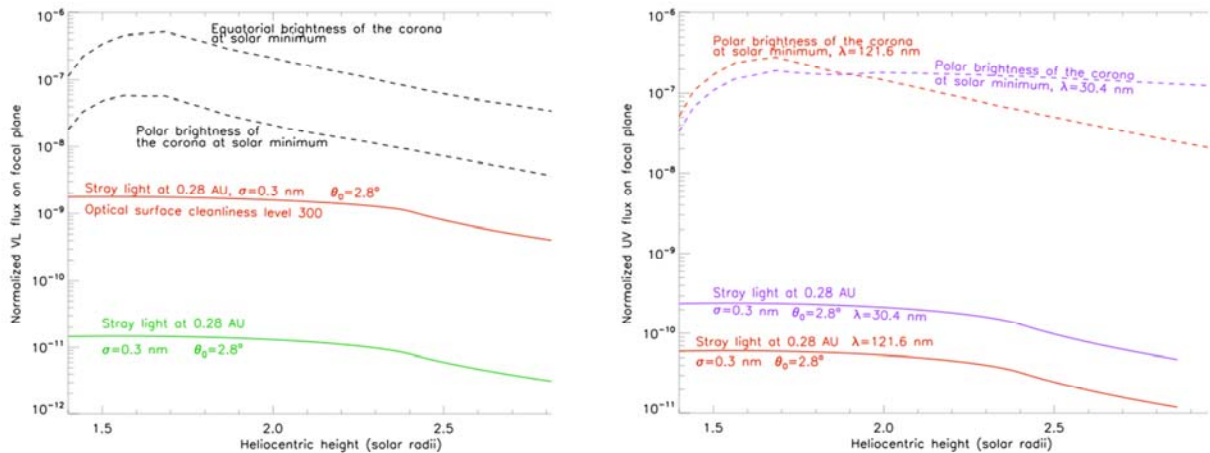


Figure 12 Estimate of the levels of stray-light on the focal plane due to the surface roughness of M1 compared to the signal from coronal structures. Left: Normalized VL flux. Right: EUV and UV fluxes.

6. CONCLUSION

METIS, the Multi *Element Telescope for Imaging and Spectroscopy*, is one of the remote-sensing instruments of Solar Orbiter consisting in an innovative coronagraph for the study and overall characterization of the solar corona. METIS is an inverted-occultation coronagraph that will image the solar corona in three different wavelengths (visible light between 590 and 650 nm, and the two Lyman- α lines of hydrogen and helium, HI at 121.6 nm and HeII at 30.4 nm) by a combination of multilayer mirror coatings and spectral bandpass filters (Figure 1).

7. ACKNOWLEDGMENT

This work has been supported by the Italian Space Agency under contract number I/043/10/0. The Authors would like to thank the team of the METIS industrial Prime Contractor THALES Alenia Space - Italy for their support.

REFERENCES

- [1] Muller, D., Marsden, R.G., StCyr, O.G., H.R. Gilbert, H.R., the Solar Orbiter Team, “*Solar Orbiter Exploring the Sun–heliosphere connection*”. Solar Phys. In press (2012).
- [2] Fineschi, S., Korendyke, C., Moses, J.D., Thomas, R.T., “*Solar ultraviolet spectro-coronagraph with toroidal varied line-space (TVLS) grating*”. SPIE 5487, 1165 (2004)
- [3] Fineschi S; “*Inverted-COR: Inverted –Occultation Coronagraph for Solar Orbiter*”; OATo Technical Report Nr 119 (2009) www.oato.inaf.it/biblioteca/pdf/TechRep119_Fineschi.pdf
- [4] Fineschi S; “*Spectra-COR: Spectral Capability for the Inverted-COR on Solar Orbiter*”; OATo Technical Report Nr 120 (2009) www.oato.inaf.it/biblioteca/pdf/TechRep120_Fineschi.pdf
- [5] Antonucci, E., Fineschi, S., et al.; “*Multi element telescope for imaging and spectroscopy (METIS)*”, SPIE 8443-08 (2012)
- [6] Uslenghi, M., et al.; “*A prototype of the UV detector for METIS on Solar Orbiter*”, SPIE 8443-128 (2012)
- [7] Capobianco, G., et al.; “*Electro-optical polarimeters for ground-based and space-based observations of the solar K-corona*”, SPIE 8450-146 (2012)
- [8] Crescenzo, G., et al.; “*Imaging polarimetry with the METIS coronagraph of the Solar Orbiter*”. SPIE 8443-129 (2012)
- [9] Pelizzo, M.G., et al.; “*Stability of extreme ultraviolet multilayer coatings to low energy proton bombardment*”, Optics Express, Vol. 19, Issue 16, pp. 14838-14844 (2011)
- [10] Landini, F., et al.; “*Optimization of the occulter for the Solar orbiter/METIS coronagraph*”, SPIE 8442-77 (2012)